INTERNATIONAL JOURNAL FOR NUMERICAL METHODS IN FLUIDS
Int. J. Numer. Meth. Fluids 2009; **61**:1201–1226
Published online 9 January 2009 in Wiley InterScience (www.interscience.wiley.com). DOI: 10.1002/fld.1991

Meshless Galerkin analysis of Stokes slip flow with boundary integral equations

Xiaolin Li*,† and Jialin Zhu

College of Mathematics and Physics, Chongqing University, Chongqing 400044, People's Republic of China

SUMMARY

This paper presents a novel meshless Galerkin scheme for modeling incompressible slip Stokes flows in 2D. The boundary value problem is reformulated as boundary integral equations of the first kind which is then converted into an equivalent variational problem with constraint. We introduce a Lagrangian multiplier to incorporate the constraint and apply the moving least-squares approximations to generate trial and test functions. In this boundary-type meshless method, boundary conditions can be implemented exactly and system matrices are symmetric. Unlike the domain-type method, this Galerkin scheme requires only a nodal structure on the bounding surface of a body for approximation of boundary unknowns. The convergence and abstract error estimates of this new approach are given. Numerical examples are also presented to show the efficiency of the method. Copyright © 2009 John Wiley & Sons, Ltd.

Received 18 July 2008; Revised 26 November 2008; Accepted 27 November 2008

KEY WORDS: Stokes equations; slip boundary condition; variational method; moving least-squares; boundary integral equations; meshless

1. INTRODUCTION

Stokes equation with slip boundary condition plays an important role in the simulation of flows with free surface, or at high angles of attack. In the flow problems, such as coating, the flow past chemically reacting walls, the classical no-slip condition of Stokes is no longer valid, for which the slip boundary condition is the appropriate physical model. The numerical solution of the practical problems of these kinds has been usually addressed with classical numerical methods, such as the finite element method (FEM) [1–5] and the boundary element method (BEM) [6–10]. However, in using these methods, meshing is a burdensome and expensive task for some problems, such as complicated boundary problems and moving boundary problems.

*Correspondence to: Xiaolin Li, Room 425, College of Mathematics and Physics, Chongqing University, Chongqing 400044, People's Republic of China.
†E-mail: lxlmath@163.com

In recent years, meshless methods have attracted considerable attention due to their ability to alleviate some of the shortcomings of the traditional procedures [11–13]. As opposed to mesh-based methods, they avoid grid generation and the approximate solution is constructed entirely based on a cluster of scattered nodes. Different kinds of meshless methods have been proposed, such as the element free Galerkin method (EFGM) [11, 14], the reproducing kernel particle method (RKPM) [15, 16], the moving least-square reproducing kernel (MLSRK) method [17], the generalized FEM [18], the finite point method [19], the point interpolation method [20], the h-p meshless method [21], the least-squares meshfree method [22], and so on.

The idea of meshless has also been applied in boundary integral equations (BIEs), such as the meshless local boundary integral equation (LBIE) method [23], the boundary node method (BNM) [24, 25], the boundary cloud method [26] and the boundary point interpolation method [27]. The LBIE method is equivalent to a sort of meshless local Petrov–Galerkin approach [28], which uses local weak forms over a local sub-domain and shape functions from the moving least-squares (MLS) approximations [11, 29]. The LBIE method, however, is not strictly a boundary method since it requires evaluation of integrals over certain surfaces (called L_s in [23]) that can be regarded as 'closure surfaces' of boundary elements. The BNM is formulated using the MLS approximations and the technique of BIEs. Compared with the LBIE method, the BNM and the rest of the BIEs-based meshless methods aforementioned can reduce the dimensionality of the original problem. Although these BIEs-based meshless methods have achieved remarkable progress in solving a broad class of boundary value problems, there still exist many problems related to their efficient implementation. Among these are difficulties in satisfying boundary conditions when their shape functions lack the delta function property, the system matrices of many boundary-type methods are non-symmetric, and the theoretical basis of these methods is just being studied and is far from completion.

In this paper we introduce a new meshless scheme for the 2-D steady incompressible Stokes equations with slip boundary condition. By combining the simple layer potential used for the Stokes problem [30, 31] with the slip boundary condition, we obtain a set of BIEs that is suitable for the interior as well as the exterior boundary value problems. Then Galerkin procedure can be applied, in which trial and test functions are constructed by the MLS approximations. Here, the problem of finding the velocity is separated from that of finding the pressure. From the analytic point of view, 2-D problems are more difficult to handle than 3-D owing to the behavior of the solution at infinite. The trial functions in the variational formulation corresponding to the BIEs of 2-D case have constraint where the Lagrangian multiplier approach [32, 33] will be introduced.

The present paper is a first attempt in applying a meshless Galerkin method of boundary type to Stokes slip flows. The main contributions of this paper can be summarized as follows:

(1) A boundary integral expression is gained for the solution of the Stokes slip flow. Then a variational formulation based on the integral equation is established.
(2) A meshless Galerkin scheme is developed for the variational formulation. Such a scheme can reduce one in dimension, thus it is especially suitable for exterior problems. Besides, this scheme yields symmetric stiffness matrix and a simplified treatment of boundary conditions.
(3) A Lagrangian multiplier is introduced to incorporate constraint conditions.
(4) A solid theoretical foundation of the present method is provided in detail. The rates of convergence for both velocity and pressure are derived in Sobolev spaces.
(5) Some selected Stokes problems are solved to illustrate the capability of the developed algorithms. The numerical results are in consistency with the theoretical analysis.

DOI: 10.1002/fld

The rest of this paper is outlined as follows. Section 2 describes the MLS approximation scheme. In Section 3, our meshless Galerkin approach is described for solving Stokes problems. The convergence of this method is stated in Section 4. Section 5 provides some numerical results. Section 6 contains conclusions.

2. THE MLS METHOD

2.1. Notations

Let Γ be a smooth, simple closed curve in the plane and let Ω and Ω' denote its interior and exterior, respectively. A generic point in $\mathbb{R}^2$ is denoted by $\mathbf{x}=(x_1, x_2)$ or $\mathbf{y}=(y_1, y_2)$.

For any point $\mathbf{x}\in\Gamma$, we use $\Re(\mathbf{x})$ to denote the influence domain of $\mathbf{x}$. Let $Q_N=\{\mathbf{x}_i\}_{i=1}^N$ be an arbitrarily chosen set of N boundary nodes $\mathbf{x}_i\in\Gamma$. The set Q_N is used for defining a finite open covering $\{\Re_i\}_{i=1}^N$ of Γ composed of N balls $\Re_i$ centered at the points $\mathbf{x}_i$, $i=1,2,\ldots,N$, where $\Re_i=\Re(\mathbf{x}_i)$ is the influence domain of $\mathbf{x}_i$.

Assume that $\kappa(\mathbf{x})$ boundary nodes lie on $\Re(\mathbf{x})$. Then, we use the notation $I_1, I_2, \ldots, I_\kappa$ to express the global sequence number of these nodes, and define $\wedge(\mathbf{x})=\{I_1, I_2, \ldots, I_\kappa\}$.

Let $w_i, i=1,2,\ldots,N$, denote weighting functions that belong to the space $C_0^\alpha(\Re_i)$, $\alpha\geqslant 0$, with the following properties:

$$w_i(\mathbf{x})>0, \quad \mathbf{x}\in\Re_i$$

$$\sum_{i\in\wedge(\mathbf{x})} w_i(\mathbf{x})=1 \quad \forall\mathbf{x}\in\Gamma$$

Besides, we use the notation

$$\Re^i=\{\mathbf{x}\in\Gamma:\mathbf{x}_i\in\Re(\mathbf{x})\}, \quad 1\leqslant i\leqslant N \tag{1}$$

for the set of boundary points whose influence domain includes the boundary node $\mathbf{x}_i$. For different boundary point $\mathbf{x}$, because $\Re(\mathbf{x})$ varies from point to point, $\Re^i\equiv\Re_i$ if and only if the radii of $\Re(\mathbf{x})$ is a constant for any $\mathbf{x}\in\Gamma$.

Let τ be an arbitrary real number, then we denote by $H^\tau(\Gamma)$ the Sobolev spaces as well as their interpolation spaces on Γ for non-integer τ [34]. Moreover, we define the following weighted Sobolev space [31]:

$$W_0^1(\Omega')=\left\{v\in\mathscr{D}'(\Omega'):\frac{v}{\sqrt{1+r^2}\ln(2+r^2)}\in L^2(\Omega'),\frac{\partial v}{\partial x_i}\in L^2(\Omega'),i=1,2\right\}$$

where $r=\sqrt{x_1^2+x_2^2}$. It is a reflexive Banach space equipped with its natural norm

$$\|v\|_{W_0^1(\Omega')}=\left(\left\|\frac{v}{\sqrt{1+r^2}\ln(2+r^2)}\right\|_{L^2(\Omega')}^2+\sum_{i=1}^2\left\|\frac{\partial v}{\partial x_i}\right\|_{L^2(\Omega')}^2\right)^{1/2}$$

Observe that all the local properties of the space $W_0^1(\Omega')$ coincide with those of the Sobolev space $H^1(\Omega')$. As a consequence, the traces of these functions on Γ satisfy the usual trace theorems.

DOI: 10.1002/fld

2.2. The MLS technique

In the MLS method, the numerical approximation starts from a cluster of scattered nodes instead of elements. Assume that $\mathbf{x}(s)\in\Gamma$, the MLS approximation for a given function v is defined as [11, 24, 29]

$$v(\mathbf{x})\approx \mathscr{M}v(\mathbf{x})=\sum_{i=1}^{N}\Phi_i(\mathbf{x})v_i \tag{2}$$

where $\mathscr{M}$ is an approximation operator, and

$$\Phi_i(\mathbf{x}(s))=\begin{cases}\sum\limits_{j=0}^{\beta}P_j(s)[\mathbf{A}^{-1}(s)\mathbf{B}(s)]_{ji}, & i\in\wedge(\mathbf{x})\\ 0, & i\notin\wedge(\mathbf{x})\end{cases} \tag{3}$$

and the matrixes $\mathbf{A}(s)$ and $\mathbf{B}(s)$ being defined by

$$\mathbf{A}(s)=\sum_{i\in\wedge(\mathbf{x}(s))}w_i(s)\mathbf{P}(s_i)\mathbf{P}^{\mathrm{T}}(s_i) \tag{4}$$

$$\mathbf{B}(s)=[w_{I_1}(s)\mathbf{P}(s_{I_1}),w_{I_2}(s)\mathbf{P}(s_{I_2}),\ldots,w_{I_\kappa}(s)\mathbf{P}(s_{I_\kappa})] \tag{5}$$

in which s is a local co-ordinate of the boundary point $\mathbf{x}$ on Γ, $\mathbf{P}(s)$ is a vector of the polynomial basis, $\beta+1$ is the number of terms of the monomials.

In order to make sense of the definition of the MLS approximations, the matrix $\mathbf{A}(s)$ must be invertible. The corresponding work can be found in References [21, 35].

For our subsequent error analysis, the following conditions will be assumed from now on:

A1. There exists a non-negative integer $\gamma\leqslant\alpha$ such that the MLS shape generating functions $\Phi_i(\mathbf{x})\in C^\gamma(\Gamma)$ and the boundary Γ is a C^γ curve.
A2. There is a constant h such that the radii of weight functions is less than h.
A3. There exist non-negative integers $K_1(\mathbf{x})\geqslant\beta$ and $K_2(\mathbf{x})$ such that for any $\mathbf{x}\in\Gamma$, there are at least $K_1(\mathbf{x})$ boundary nodes, and at most $K_2(\mathbf{x})$ boundary nodes lie on $\Re(\mathbf{x})$.
A4. There is a uniform bound of the MLS shape function and its derivatives. Namely, constants $C_{\Phi1}$ and $C_{\Phi2}$ are independent of h such that $C_{\Phi1}h^{-j}\leqslant\sum_{|\lambda|=j}\|\partial^\lambda\Phi_i(\mathbf{x})\|_{L^\infty(\Gamma)}\leqslant C_{\Phi2}h^{-j}$, $0\leqslant j\leqslant\gamma$, $1\leqslant i\leqslant N$.

Remark 2.1
From Reference [21], if monomials P_j $(j=0,1,\ldots,\beta)$ and weight functions w_i $(1\leqslant i\leqslant N)$ are γ times continuously differentiable, then $\Phi_i\in C^\gamma(\Gamma)$.

Remark 2.2
Assumption (A3) is quite natural since otherwise as the number of boundary nodes lying on a local area increases, the shape functions tend to be more and more linearly dependent in the local area.

We list below some properties of the MLS shape generating functions Φ_i.

Property 2.1 (*Liu et al.* [17])
$\sum_{i=1}^{N}D^j\Phi_i(s)(s_i-s)^k=k!\delta_{jk}$, $0\leqslant j\leqslant\gamma$, $0\leqslant k\leqslant\beta$.

DOI: 10.1002/fld

Property 2.2
$\Phi_i(\mathbf{x}) \in C_0^{\gamma}(\Re^i)$, $1 \leqslant i \leqslant N$.

This property follows immediately from the fact that the weight functions $w_i(\mathbf{x})$ have compact supports.

Property 2.3
There exists a constant C independent of h such that

$$\|\Phi_i(\mathbf{x})\|_{H^k(\Gamma)} \leqslant Ch^{m-k} \|\Phi_i(\mathbf{x})\|_{H^m(\Gamma)}, \quad 1 \leqslant i \leqslant N, \ -\gamma \leqslant m \leqslant k, \ 0 \leqslant k \leqslant \gamma \tag{6}$$

Proof
According to Assumption (A4), we have

$$|\Phi_i|^2_{H^k(\Gamma)} = \int_\Gamma \sum_{|\lambda|=k} |D^\lambda \Phi_i(\mathbf{x})|^2 \, \mathrm{d}S_{\mathbf{x}} \leqslant \int_\Gamma (C_{k2} h^{-k})^2 \, \mathrm{d}S_{\mathbf{x}}, \quad 0 \leqslant k \leqslant \gamma$$

$$|\Phi_i|^2_{H^m(\Gamma)} = \int_\Gamma \sum_{|\lambda|=m} |D^\lambda \Phi_i(\mathbf{x})|^2 \, \mathrm{d}S_{\mathbf{x}} \geqslant \int_\Gamma (C_{m1} h^{-m})^2 \, \mathrm{d}S_{\mathbf{x}}, \quad 0 \leqslant m \leqslant \gamma$$

thus

$$|\Phi_i|_{H^k(\Gamma)} \leqslant Ch^{m-k} |\Phi_i|_{H^m(\Gamma)}, \quad 0 \leqslant m \leqslant k \leqslant \gamma \tag{7}$$

On the other hand,

$$\|\Phi_i\|^2_{H^0(\Gamma)} \leqslant \|\Phi_i\|_{H^m(\Gamma)} \|\Phi_i\|_{H^{-m}(\Gamma)} \leqslant Ch^m \|\Phi_i\|_{H^m(\Gamma)} \|\Phi_i\|_{H^0(\Gamma)}, \quad -\gamma \leqslant m \leqslant 0 \tag{8}$$

Hence, applying (7) and (8) yields

$$\|\Phi_i\|_{H^k(\Gamma)} \leqslant Ch^{-k} \|\Phi_i\|_{H^0(\Gamma)} \leqslant Ch^{m-k} \|\Phi_i\|_{H^m(\Gamma)}, \quad -\gamma \leqslant m \leqslant 0, \ 0 \leqslant k \leqslant \gamma \tag{9}$$

By gathering (7)–(9) we have ended the proof. □

The following approximation theorem gives an approximation estimate for the MLS approximations, which is central to the convergence proof of our meshless Galerkin method.

Theorem 2.1
Assume that $v \in H^{\gamma+1}(\Gamma)$. Let $\mathscr{M}v = \sum_{i=1}^N \Phi_i v_i$, then

$$\|v - \mathscr{M}v\|_{H^k(\Gamma)} \leqslant Ch^{\gamma+1-k} \|v\|_{H^{\gamma+1}(\Gamma)}, \quad 0 \leqslant k \leqslant \gamma \tag{10}$$

where the constant C is independent of h.

This result was proved by Han and Meng [15] in the context of the RKPM, and by Liu *et al.* [17] in the MLSRK approximation method. The proof of the theorem above is exactly along the same lines and thus we shall omit the proof.

DOI: 10.1002/fld

3. MESHLESS GALERKIN SCHEME FOR STOKES EQUATIONS USING BIEs

In this section, a meshless Galerkin method for the approximation of the incompressible Stokes equations is introduced. In this approach, meshless shape functions are constructed with the MLS technique and are used in a Galerkin setting for the approximation of the weak form of BIEs.

3.1. BIEs and variational formulation

We consider the interior and exterior Stokes problems as

$$-\mu\Delta\mathbf{u}+\nabla p=0 \quad \text{in } \Omega \text{ or } \Omega' \tag{11}$$

$$\nabla\cdot\mathbf{u}=0 \quad \text{in } \Omega \text{ or } \Omega' \tag{12}$$

$$\mathbf{u}\cdot\mathbf{n}=g \quad \text{on } \Gamma \tag{13}$$

$$\mathbf{n}\cdot\sigma(\mathbf{u},p)\cdot\boldsymbol{\tau}=0 \quad \text{on } \Gamma \tag{14}$$

where $\mathbf{u}=(u_1,u_2)$ is the velocity of the fluid, p is the pressure, μ is the constant positive viscosity coefficient, $\mathbf{n}=(n_1,n_2)$ is the unit exterior normal to Γ, $\boldsymbol{\tau}=(\tau_1,\tau_2)$ is the tangent vector to Γ, g is a given function, and $\sigma(\mathbf{u},p)$ is the stress tensor of the form

$$(\sigma(\mathbf{u},p))_{ij}=-p\delta_{ij}+2\mu\varepsilon_{ij}(\mathbf{u}) \tag{15}$$

where δ_{ij} is the Kronecker symbol and

$$\varepsilon_{ij}(\mathbf{u})=(\varepsilon(\mathbf{u}))_{ij}=\tfrac{1}{2}(u_{i,j}+u_{j,i})$$

is the deformation tensor. In the case of the exterior problem, we append to (11)–(14) the following condition at infinity:

$$|u_i(\mathbf{x})|=O(1), \quad i=1,2, \quad |\mathbf{x}|\to\infty$$

Condition (13) is an essential boundary condition, whereas condition (14) is a natural one. The incompressibility condition (12) implies the following compatibility condition:

$$\int_\Gamma g(\mathbf{x})\,\mathrm{d}S_{\mathbf{x}}=0$$

which must be satisfied by datum g from (13).

In order to derive a proper weak formulation of problem (11)–(14), we introduce Sobolev space

$$V=\{\mathbf{v}\in(H^1(\Omega))^2\cup(W_0^1(\Omega'))^2,\nabla\cdot\mathbf{v}=0\}$$

From Green's formula and the boundary condition (14), we have

$$\begin{aligned}
&2\mu\int_\Omega\varepsilon(\mathbf{u})\cdot\varepsilon(\mathbf{v})\,\mathrm{d}\mathbf{x}-\int_\Omega(-\mu\Delta\mathbf{u}+\operatorname{grad}p)\cdot\mathbf{v}\,\mathrm{d}\mathbf{x}\\
&=\int_\Gamma\mathbf{n}\cdot\sigma(\mathbf{u},p)\cdot\mathbf{v}\,\mathrm{d}S_{\mathbf{x}}\\
&=\int_\Gamma(\mathbf{n}\cdot\sigma(\mathbf{u},p)\cdot\mathbf{n})(\mathbf{v}\cdot\mathbf{n})\,\mathrm{d}S_{\mathbf{x}}
\end{aligned}$$

DOI: 10.1002/fld

$$
\begin{aligned}
&2\mu\int_{\Omega'}\varepsilon(\mathbf{u})\cdot\varepsilon(\mathbf{v})\,\mathrm{d}\mathbf{x}-\int_{\Omega'}(-\mu\Delta\mathbf{u}+\operatorname{grad}p)\cdot\mathbf{v}\,\mathrm{d}\mathbf{x}\\
&\quad=-\int_{\Gamma}\mathbf{n}\cdot\sigma(\mathbf{u},p)\cdot\mathbf{v}\,\mathrm{d}S_{\mathbf{x}}\\
&\quad=-\int_{\Gamma}(\mathbf{n}\cdot\sigma(\mathbf{u},p)\cdot\mathbf{n})(\mathbf{v}\cdot\mathbf{n})\,\mathrm{d}S_{\mathbf{x}}
\end{aligned}
$$

for any $\mathbf{u},\mathbf{v}\in V$. We then get, by adding the above two formulas,

$$
2\mu\int_{\Omega\cup\Omega'}\varepsilon(\mathbf{u})\cdot\varepsilon(\mathbf{v})\,\mathrm{d}\mathbf{x}=\int_{\Gamma}(\mathbf{t}\cdot\mathbf{n})(\mathbf{v}\cdot\mathbf{n})\,\mathrm{d}S_{\mathbf{x}}\quad\forall\mathbf{u},\mathbf{v}\in V \tag{16}
$$

where $\mathbf{t}$ stands for the jump through Γ of $\mathbf{n}\cdot\sigma(\mathbf{u},p)$

$$
\mathbf{t}=[\mathbf{n}\cdot\sigma(\mathbf{u},p)]=(\mathbf{n}\cdot\sigma(\mathbf{u},p))_{\Gamma}^{\mathrm{int}}-(\mathbf{n}\cdot\sigma(\mathbf{u},p))_{\Gamma}^{\mathrm{ext}} \tag{17}
$$

The simple layer potential corresponding to Stokes equation [30, 31] can be adapted to combining the boundary condition (14), if we take the decomposition of the fundamental solution into orthogonal directions

$$
\begin{aligned}
u_i(\mathbf{y})&=\int_{\Gamma}\mathbf{t}(\mathbf{x})\cdot\mathbf{U}_i(\mathbf{x},\mathbf{y})\,\mathrm{d}S_{\mathbf{x}}+\xi_i\\
&=\int_{\Gamma}\mathbf{t}(\mathbf{x})\cdot((\mathbf{U}_i\cdot\mathbf{n})\mathbf{n}+(\mathbf{U}_i\cdot\boldsymbol{\tau})\boldsymbol{\tau})\,\mathrm{d}S_{\mathbf{x}}+\xi_i\\
&=\int_{\Gamma}(\mathbf{t}(\mathbf{x})\cdot\mathbf{n}(\mathbf{x}))(\mathbf{U}_i(\mathbf{x},\mathbf{y})\cdot\mathbf{n}(\mathbf{x}))\,\mathrm{d}S_{\mathbf{x}}+\xi_i\\
p(\mathbf{y})&=-\int_{\Gamma}\mathbf{t}(\mathbf{x})\cdot\mathbf{P}(\mathbf{x},\mathbf{y})\,\mathrm{d}S_{\mathbf{x}}\\
&=-\int_{\Gamma}\mathbf{t}(\mathbf{x})\cdot((\mathbf{P}\cdot\mathbf{n})\mathbf{n}+(\mathbf{P}\cdot\boldsymbol{\tau})\boldsymbol{\tau})\,\mathrm{d}S_{\mathbf{x}}\\
&=-\int_{\Gamma}(\mathbf{t}(\mathbf{x})\cdot\mathbf{n}(\mathbf{x}))(\mathbf{P}(\mathbf{x},\mathbf{y})\cdot\mathbf{n}(\mathbf{x}))\,\mathrm{d}S_{\mathbf{x}}
\end{aligned}
$$

in which $\boldsymbol{\xi}=(\xi_1,\xi_2)$ is a constant vector, $\mathbf{U}_i=(U_{i1},U_{i2})$ and $\mathbf{P}=(P_1,P_2)$ are the fundamental solutions of Stokes equation

$$
U_{ij}(\mathbf{x},\mathbf{y})=\frac{1}{4\pi\mu}\left[\delta_{ij}\ln\frac{1}{|\mathbf{x}-\mathbf{y}|}+\frac{(x_i-y_i)(x_j-y_j)}{|\mathbf{x}-\mathbf{y}|^2}\right],\quad i,j=1,2 \tag{18}
$$

$$
P_j(\mathbf{x},\mathbf{y})=\frac{x_j-y_j}{2\pi|\mathbf{x}-\mathbf{y}|^2},\quad j=1,2 \tag{19}
$$

DOI: 10.1002/fld

Putting $q=\mathbf{t}\cdot\mathbf{n}$, we finally obtain the expression of the solution of problem (11)–(14) as

$$u_i(\mathbf{y})=\sum_{j=1}^{2}\int_\Gamma q(\mathbf{x})U_{ij}(\mathbf{x},\mathbf{y})n_j(\mathbf{x})\,\mathrm{d}S_\mathbf{x}+\xi_i,\quad \mathbf{y}\in\mathbb{R}^2,\ \ i=1,2 \tag{20}$$

$$p(\mathbf{y})=-\sum_{j=1}^{2}\int_\Gamma q(\mathbf{x})P_j(\mathbf{x},\mathbf{y})n_j(\mathbf{x})\,\mathrm{d}S_\mathbf{x},\quad \mathbf{y}\in\mathbb{R}^2/\Gamma \tag{21}$$

in which the intermediate variable $q(\mathbf{x})$ is the jump through Γ of normal stress component $\mathbf{n}\cdot\sigma(\mathbf{u},p)\cdot\mathbf{n}$.

In addition to the integral equations above, we have to consider the compatibility condition. Taking $\mathbf{v}=\boldsymbol{\xi}\in\mathbb{R}^2\subset V$ in formula (16), we derive the compatibility condition as follows:

$$\int_\Gamma q\sum_{j=1}^{2}\xi_j n_j\,\mathrm{d}S=0\quad \forall\boldsymbol{\xi}=(\xi_1,\xi_2)\in\mathbb{R}^2 \tag{22}$$

Now giving

$$g\in H_0^{1/2}(\Gamma)=\left\{\phi\in H^{1/2}(\Gamma),\int_\Gamma\phi\,\mathrm{d}S=0\right\}$$

the following integral equations of the first kind define a continuous mapping $g\to q$:

$$g(\mathbf{y})=\sum_{i=1}^{2}n_i(\mathbf{y})\left(\sum_{j=1}^{2}\int_\Gamma q(\mathbf{x})U_{ij}(\mathbf{x},\mathbf{y})n_j(\mathbf{x})\,\mathrm{d}S_\mathbf{x}+\xi_i\right),\quad \mathbf{y}\in\Gamma \tag{23}$$

We emphasize that (23) is suitable for the solution of the exterior as well as the interior Stokes problem.

As the pressure p could be determined within an arbitrary additive constant, we know from (15) and (17) that $\mathbf{t}\in(H^{-1/2}(\Gamma))^2$ could only be determined within a vector proportional to the normal $\mathbf{n}$ to Γ; so we see that $q\in H^{-1/2}(\Gamma)$ can be determined up to an arbitrary constant. We then consider the inverse problem, giving

$$q\in H_{00}^{-1/2}(\Gamma)=\left\{\phi\in H^{-1/2}(\Gamma)/\mathbb{R},\int_\Gamma\phi\sum_{j=1}^{2}\xi_j n_j\,\mathrm{d}S=0\ \forall\boldsymbol{\xi}\in\mathbb{R}^2\right\}$$

From (16) we get a variational formula

$$2\mu\int_{\Omega\cup\Omega'}\varepsilon(\mathbf{u})\cdot\varepsilon(\mathbf{v})\,\mathrm{d}\mathbf{x}=\int_\Gamma q\sum_{j=1}^{2}v_j n_j\,\mathrm{d}S\quad \forall\mathbf{v}=(v_1,v_2)\in V \tag{24}$$

The bilinear form

$$a(\mathbf{u},\mathbf{v})=2\mu\int_{\Omega\cup\Omega'}\varepsilon(\mathbf{u})\cdot\varepsilon(\mathbf{v})\,\mathrm{d}\mathbf{x}=\mu\sum_{i=1}^{2}\int_{\Omega\cup\Omega'}\mathrm{grad}\,u_i\cdot\mathrm{grad}\,v_i\,\mathrm{d}\mathbf{x}$$

is coercive on V, since here the semi-norm is equivalent to the norm in V [31], i.e.

$$a(\mathbf{u},\mathbf{u})=\mu\sum_{i=1}^{2}\int_{\Omega\cup\Omega'}|\mathrm{grad}\,u_i|^2\,\mathrm{d}\mathbf{x}=\mu|\mathbf{u}|_V^2\geqslant C\|\mathbf{u}\|_V^2,\quad C>0 \tag{25}$$

DOI: 10.1002/fld

Moreover, $\int_\Gamma q \sum_{j=1}^{2} v_j n_j \, \mathrm{d}S$ is a continuous linear functional on V. Therefore, by Lax–Milgram theorem there exists a unique function $\mathbf{u} \in V$ that satisfies the variational equation (24); then by Trace theorem we can get $g \in H_0^{1/2}(\Gamma)$.

To summarize, we have shown the following theorem.

Theorem 3.1
The BIE (23) defines an isomorphism from $H_0^{1/2}(\Gamma)$ onto $H_{00}^{-1/2}(\Gamma)$, which admits the following variational problem:

$$\begin{aligned} &\text{Find } q \in H_{00}^{-1/2}(\Gamma) \quad \text{such that } \forall q' \in H_{00}^{-1/2}(\Gamma) \\ &b(q, q') = \langle g, q' \rangle \end{aligned} \tag{26}$$

with

$$b(q, q') = \sum_{i,j=1}^{2} \int_\Gamma \int_\Gamma U_{ij}(\mathbf{x}, \mathbf{y}) n_j(\mathbf{x}) q(\mathbf{x}) n_i(\mathbf{y}) q'(\mathbf{y}) \, \mathrm{d}S_{\mathbf{x}} \, \mathrm{d}S_{\mathbf{y}}$$

$$\langle g, q' \rangle = \int_\Gamma g(\mathbf{y}) q'(\mathbf{y}) \, \mathrm{d}S_{\mathbf{y}}, \quad g \in H_0^{1/2}(\Gamma), \quad q' \in H_{00}^{-1/2}(\Gamma)$$

Theorem 3.2
Problem (26) has one and only one solution.

Proof
Let $\mathbf{u}$ and $\tilde{\mathbf{u}}$ be the solutions of (24) respectively corresponding to q and $\tilde{q}$; if their traces on Γ verify the integral equation (23), then we have by the construction

$$\begin{aligned} b(q, \tilde{q}) &= \sum_{i,j=1}^{2} \int_\Gamma \int_\Gamma U_{ij}(\mathbf{x}, \mathbf{y}) n_j(\mathbf{x}) q(\mathbf{x}) n_i(\mathbf{y}) \tilde{q}(\mathbf{y}) \, \mathrm{d}S_{\mathbf{x}} \, \mathrm{d}S_{\mathbf{y}} \\ &= \langle \mathbf{u} \cdot \mathbf{n}, \tilde{q} \rangle = \langle \tilde{\mathbf{u}} \cdot \mathbf{n}, q \rangle \\ &= \mu \sum_{i=1}^{2} \int_{\Omega \cup \Omega'} \operatorname{grad} u_i \cdot \operatorname{grad} \tilde{u}_i \, \mathrm{d}\mathbf{x} \end{aligned}$$

Besides, substituting (25) into (24) and (26), we find

$$b(q, q) = \mu \sum_{i=1}^{2} \int_{\Omega \cup \Omega'} |\operatorname{grad} u_i|^2 \, \mathrm{d}\mathbf{x} = a(\mathbf{u}, \mathbf{u}) \geqslant C \|\mathbf{u}\|_V^2 \geqslant C \|q\|_{H_{00}^{-1/2}(\Gamma)}^2$$

due to the already shown isomorphism between $\mathbf{u}$ and q defined by (24).

Thus the bilinear form $b(\cdot, \cdot)$ is symmetrical and positive definite on $H_{00}^{-1/2}(\Gamma)$. In consequence, the Lax–Milgram theorem is applied, and we conclude that the variational problem (26) has a unique solution $q \in H_{00}^{-1/2}(\Gamma)$. □

DOI: 10.1002/fld

Remark 3.1
Once q is obtained from variational problem (26), the solution $(\mathbf{u}, p)$ of problem (11)–(14) will be determined by expressions (20) and (21). They are unique in the space $(H^1(\Omega))^2 \times (L^2(\Omega)/\mathbb{R})$ or $(W_0^1(\Omega'))^2 \times L^2(\Omega')$.

3.2. Approximation

Let

$$V_h(\Gamma) = \text{span}\{\Phi_i, 1 \leqslant i \leqslant N\}$$

the basis functions Φ_i defined in (3). Observe that, since $\Phi_i(\mathbf{x}) \in C_0^\gamma(\Re^i)$, $\mathbf{x} \in \Gamma$, then $\Phi_i(\mathbf{x}) \in C^\gamma(\Gamma)$, $1 \leqslant i \leqslant N$. Thus, if $-\frac{1}{2} \leqslant m \leqslant \gamma$, one gets $\Phi_i(\mathbf{x}) \in H^m(\Gamma) \subset H^{-1/2}(\Gamma)$. Besides, we have from Property 2.1 that the constant is included in the space $V_h(\Gamma)$. Let

$$\overset{\circ}{V}_h(\Gamma) = \left\{ f \in V_h(\Gamma), \int_\Gamma f \sum_{j=1}^{2} \xi_j n_j \, \mathrm{d}S = 0, \forall \boldsymbol{\xi} \in \mathbb{R}^2 \right\}$$

then the variational problem (26) can be approximated by

$$\begin{aligned} &\text{Find } q_h \in \overset{\circ}{V}_h/\mathbb{R} \quad \text{such that } \forall q' \in \overset{\circ}{V}_h/\mathbb{R} \\ &b(q_h, q') = \langle g, q' \rangle \end{aligned} \tag{27}$$

In this way, we must take into account the constraint

$$\int_\Gamma q_h \sum_{j=1}^{2} \xi_j n_j \, \mathrm{d}S = 0 \quad \forall \boldsymbol{\xi} \in \mathbb{R}^2 \tag{28}$$

in the process of approximation. For the convenience of numerical implementation, we prefer another approach: By introducing a Lagrangian multiplier to replace the constraint (28), we define a bilinear form

$$e(\boldsymbol{\xi}, q_h) = \int_\Gamma q_h \sum_{j=1}^{2} \xi_j n_j \, \mathrm{d}S \quad \forall q_h \in V_h, \ \ \boldsymbol{\xi} \in \mathbb{R}^2 \tag{29}$$

then solve another variational problem as the following instead of (27):

$$\begin{aligned} &\text{Find } (q_h, \boldsymbol{\xi}) \in (V_h/\mathbb{R}) \times \mathbb{R}^2 \quad \text{such that } \forall (q', \boldsymbol{\xi}') \in (V_h/\mathbb{R}) \times \mathbb{R}^2 \\ &b(q_h, q') + e(\boldsymbol{\xi}, q') = \langle g, q' \rangle \\ &e(\boldsymbol{\xi}', q_h) = 0 \end{aligned} \tag{30}$$

Theorem 3.3
The variational problem (27) has one and only one solution $q_h \in \overset{\circ}{V}_h/\mathbb{R}$ and there exists a constant vector $\boldsymbol{\xi} \in \mathbb{R}^2$ such that $(q_h, \boldsymbol{\xi})$ is the unique solution of variational problem (30). Besides, there

DOI: 10.1002/fld

exists a constant C such that

$$\|q-q_h\|_{H^{-1/2}(\Gamma)/\mathbb{R}} \leqslant C \left\{ \inf_{q'\in V_h/\mathbb{R}} \|q-q'\|_{H^{-1/2}(\Gamma)/\mathbb{R}} + \inf_{\xi'\in\mathbb{R}^2} \|\xi-\xi'\|_{\mathbb{R}^2} \right\}$$
$$= C \inf_{q'\in V_h/\mathbb{R}} \|q-q'\|_{H^{-1/2}(\Gamma)/\mathbb{R}} \tag{31}$$

Proof
According to Brezzi [32] and Girault and Raviart [33], we need to verify just the following two assumptions:

(i) There exists a constant $C^*>0$ such that

$$b(q_h,q_h) \geqslant C^* \|q_h\|^2_{H^{-1/2}(\Gamma)/\mathbb{R}} \quad \forall q_h \in V_h/\mathbb{R}$$

(ii) There exists a constant $C^{**}>0$ such that

$$\sup_{q_h\in V_h/\mathbb{R}} \frac{e(\xi,q_h)}{\|q_h\|_{V_h/\mathbb{R}}} \geqslant C^{**}\|\xi\|_{\mathbb{R}^2} \quad \forall \xi\in\mathbb{R}^2$$

The first assumption is satisfied because of the result of Theorem 3.2, since $q_h \in V_h/\mathbb{R}$ implies $q_h \in H^{-1/2}(\Gamma)/\mathbb{R}$. For the second assumption, take $q_h = \xi\cdot\mathbf{n}$ to obtain

$$\sup_{q_h\in V_h/\mathbb{R}} \frac{e(\xi,q_h)}{\|q_h\|_{V_h/\mathbb{R}}} \geqslant \frac{\int_\Gamma (\xi\cdot\mathbf{n})^2\,\mathrm{d}S}{\|\xi\cdot\mathbf{n}\|_{V_h/\mathbb{R}}} \geqslant \frac{\|\xi\cdot\mathbf{n}\|^2_{L^2(\Gamma)}}{C_1\|\xi\cdot\mathbf{n}\|_{L^2(\Gamma)}} = \frac{1}{C_1}\|\xi\cdot\mathbf{n}\|_{L^2(\Gamma)} \geqslant C^{**}\|\xi\|_{\mathbb{R}^2}$$

Thus the proof is complete. □

On $V_h(\Gamma)/\mathbb{R}$, the Galerkin approximation q_h of the real solution q may be read as

$$q_h(\mathbf{x}) = \sum_{i=1}^{N} \Phi_i(\mathbf{x}) q_i \tag{32}$$

Substituting (32) into (30), by virtue of Property 2.2, one gets

$$\begin{Bmatrix} [a_{ji}] & [c_{jk}] \\ [b_{ki}] & [0] \end{Bmatrix} \begin{Bmatrix} \{q_i\} \\ \{\xi_k\} \end{Bmatrix} = \begin{Bmatrix} \{f_j\} \\ \{0\} \end{Bmatrix}, \quad i,j=1,2,\ldots,N, \;\; k=1,2 \tag{33}$$

where

$$a_{ji} = \sum_{m,l=1}^{2} \int_{\Re^j}\int_{\Re^i} U_{ml}(\mathbf{x},\mathbf{y}) n_l(\mathbf{x}) \Phi_i(\mathbf{x}) n_m(\mathbf{y}) \Phi_j(\mathbf{y})\,\mathrm{d}S_{\mathbf{x}}\,\mathrm{d}S_{\mathbf{y}}$$

$$c_{jk} = b_{kj} = \int_{\Re^j} \Phi_j(\mathbf{y}) n_k(\mathbf{y})\,\mathrm{d}S_{\mathbf{y}}$$

$$f_j = \int_{\Re^j} g(\mathbf{y})\Phi_j(\mathbf{y})\,\mathrm{d}S_{\mathbf{y}}$$

DOI: 10.1002/fld

in which $\Re^j$ and $\Re^i$ are defined by (1), and are parts of the boundary Γ. As in the EFGM [11] and the BNM [24], these integrations can be numerically calculated by employing a cell structure.

Remark 3.2
Since the cell can be of any shape and the only restriction is that the unions of all cells equal the integral area, the concept of cell is quite different from that of an element in the BEM. Thus, the proposed method is a boundary-type meshless method.

Remark 3.3
The boundary function $g(\mathbf{y})$ are multiplied by $\Phi_j(\mathbf{y})$ and integrated on Γ. As a consequence, boundary conditions can be implemented accurately despite of the fact that the MLS approximations lack the delta function property.

Remark 3.4
The system matrix in (33) is symmetric.

4. ERROR ESTIMATES

In this section, we will prove that the result obtained using our meshless Galerkin method converges to the solution of the problem (11)–(14) gradually. First, for the MLS Galerkin solution q_h of (27), we have the following error estimate.

Theorem 4.1
Let q and q_h be the solutions of the problems (26) and (27), respectively. If $q \in H_{00}^{-1/2}(\Gamma) \cap (H^{m+1}(\Gamma)/\mathbb{R})$, then

$$\|q-q_h\|_{H^{-1/2}(\Gamma)/\mathbb{R}} \leqslant Ch^{m+3/2}\|q\|_{H^{m+1}(\Gamma)/\mathbb{R}}, \quad 0 \leqslant m \leqslant \gamma \tag{34}$$

where C is a constant independent of h.

Proof
According to Theorem 3.3, we have

$$\|q-q_h\|_{H^{-1/2}(\Gamma)/\mathbb{R}} \leqslant C \inf_{q' \in V_h/\mathbb{R}} \|q-q'\|_{H^{-1/2}(\Gamma)/\mathbb{R}} \tag{35}$$

Since q' is an arbitrary element in $V_h/\mathbb{R}$, let

$$q' = S_h q$$

where S_h denotes a projection from $L^2(\Gamma)/\mathbb{R}$ onto $V_h/\mathbb{R}$. Note that $q_h \neq S_h q$. Hence,

$$\|q-q_h\|_{H^{-1/2}(\Gamma)/\mathbb{R}} \leqslant C\|q-S_h q\|_{H^{-1/2}(\Gamma)/\mathbb{R}} \tag{36}$$

From Property 2.1 we have $\mathscr{M}c = c$ for any $c \in \mathbb{R}$; thus, applying Theorem 2.1 yields

$$\|q-\mathscr{M}q\|_{H^k(\Gamma)/\mathbb{R}} \leqslant Ch^{m+1-k}\|q\|_{H^{m+1}(\Gamma)/\mathbb{R}}, \quad 0 \leqslant k \leqslant m \leqslant \gamma$$

Then

$$\|q-S_h q\|_{H^0(\Gamma)/\mathbb{R}} \leqslant \|q-\mathscr{M}q\|_{H^0(\Gamma)/\mathbb{R}} \leqslant Ch^{m+1}\|q\|_{H^{m+1}(\Gamma)/\mathbb{R}}, \quad 0 \leqslant m \leqslant \gamma \tag{37}$$

DOI: 10.1002/fld

Thus, according to a classical duality argument we deduce

$$\begin{aligned}\|q-S_hq\|_{H^{-1}(\Gamma)/\mathbb{R}} &= \sup_{f\in H^1(\Gamma)/\mathrm{R}} \frac{\langle q-S_hq, f\rangle}{\|f\|_{H^1(\Gamma)/\mathbb{R}}}\\ &= \sup_{f\in H^1(\Gamma)/\mathbb{R}} \frac{\langle q-S_hq, f-S_hf\rangle}{\|f\|_{H^1(\Gamma)/\mathbb{R}}}\\ &\leqslant \sup_{f\in H^1(\Gamma)/\mathbb{R}} \frac{\|q-S_hq\|_{H^0(\Gamma)/\mathbb{R}}\|f-S_hf\|_{H^0(\Gamma)/\mathbb{R}}}{\|f\|_{H^1(\Gamma)/\mathbb{R}}}\\ &\leqslant Ch^{m+2}\|q\|_{H^{m+1}(\Gamma)/\mathbb{R}}, \quad 0\leqslant m\leqslant\gamma\end{aligned}$$

Hence, using an interpolation theorem of Sobolev spaces [34] leads to

$$\begin{aligned}\|q-S_hq\|_{H^{-1/2}(\Gamma)/\mathbb{R}} &\leqslant \|q-S_hq\|^{1/2}_{H^0(\Gamma)/\mathbb{R}}\|q-S_hq\|^{1/2}_{H^{-1}(\Gamma)/\mathbb{R}}\\ &\leqslant Ch^{m+3/2}\|q\|_{H^{m+1}(\Gamma)/\mathbb{R}}, \quad 0\leqslant m\leqslant\gamma\end{aligned} \tag{38}$$

Finally, substituting (38) into (36) ends the proof. □

Theorem 4.2
Let $\frac{1}{2}\leqslant k\leqslant\gamma+2$, then under conditions of Theorem 4.1,

$$\|q-q_h\|_{H^{-k}(\Gamma)/\mathbb{R}}\leqslant Ch^{m+1+k}\|q\|_{H^{m+1}(\Gamma)/\mathbb{R}}, \quad 0\leqslant m\leqslant\gamma \tag{39}$$

Proof
Write Aq for the right hand of (23), then operator A has the symmetry and A is an isomorphism from $H^{k-1}(\Gamma)/\mathbb{R}$ onto $H^k_0(\Gamma)$, where

$$H^k_0(\Gamma)=\left\{\phi\in H^k(\Gamma), \int_\Gamma \phi\,\mathrm{d}S=0\right\}$$

Using the dual theory, we have

$$\|q-q_h\|_{H^{-k}(\Gamma)/\mathbb{R}}=\sup_{\varphi\in H^k_0(\Gamma)}\frac{|\langle q-q_h,\varphi\rangle|}{\|\varphi\|_{H^k_0(\Gamma)}}=\sup_{\varphi\in H^k_0(\Gamma)}\frac{|\langle A(q-q_h),A^{-1}\varphi\rangle|}{\|\varphi\|_{H^k_0(\Gamma)}} \tag{40}$$

Clearly we have

$$\|A^{-1}\varphi\|_{H^{k-1}(\Gamma)/\mathbb{R}}\leqslant C\|\varphi\|_{H^k_0(\Gamma)}, \quad k\geqslant\tfrac{1}{2} \tag{41}$$

On the other hand,

$$\langle A(q-q_h),A^{-1}\varphi\rangle=\langle A(q-q_h),A^{-1}\varphi-S_h(A^{-1}\varphi)\rangle+\langle A(q-q_h),S_h(A^{-1}\varphi)\rangle$$

where S_h denotes a projection from $L^2(\Gamma)/\mathbb{R}$ onto $V_h/\mathbb{R}$. From (26) and (27) we get

$$\langle A(q-q_h),S_h(A^{-1}\varphi)\rangle=0$$

DOI: 10.1002/fld

Besides, according to the continuity of the bilinear form $b(\cdot,\cdot)=\langle A\cdot,\cdot\rangle$ and using Theorem 4.1 and (38), we obtain

$$\begin{aligned}\langle A(q-q_h), A^{-1}\varphi - S_h(A^{-1}\varphi)\rangle &\leqslant C\|q-q_h\|_{H^{-1/2}(\Gamma)/\mathbb{R}}\|A^{-1}\varphi - S_h(A^{-1}\varphi)\|_{H^{-1/2}(\Gamma)/\mathbb{R}}\\ &\leqslant Ch^{m+1+k}\|q\|_{H^{m+1}(\Gamma)/\mathbb{R}}\|A^{-1}\varphi\|_{H^{k-1}(\Gamma)/\mathbb{R}}\end{aligned}$$

with $\frac{1}{2}\leqslant k\leqslant \gamma+2$ and $0\leqslant m\leqslant\gamma$. Thus

$$\langle A(q-q_h), A^{-1}\varphi\rangle \leqslant Ch^{m+1+k}\|q\|_{H^{m+1}(\Gamma)/\mathbb{R}}\|A^{-1}\varphi\|_{H^{k-1}(\Gamma)/\mathbb{R}} \tag{42}$$

Consequently, the conclusion of the theorem follows from (40)–(42). □

Remark 4.1
Theorem 4.2 shows the highest rate of the convergence achieved by our Galerkin method for the density function q as $O(h^{2\gamma+3})$ in $H^{-\gamma-2}(\Gamma)/\mathbb{R}$.

Now we are in a position to estimate an error between the solution $(\mathbf{u}, p)$ given by (20) and (21) and the approximate solution $(\mathbf{u}_h, p_h)$ given by the following expression:

$$u_{hi}(\mathbf{y}) = \sum_{j=1}^{2}\int_\Gamma q_h(\mathbf{x})U_{ij}(\mathbf{x},\mathbf{y})n_j(\mathbf{x})\,\mathrm{d}S_{\mathbf{x}} + \xi_i, \quad \mathbf{y}\in\mathbb{R}^2, \ \ i=1,2 \tag{43}$$

$$p_h(\mathbf{y}) = -\sum_{j=1}^{2}\int_\Gamma q_h(\mathbf{x})P_j(\mathbf{x},\mathbf{y})n_j(\mathbf{x})\,\mathrm{d}S_{\mathbf{x}}, \quad \mathbf{y}\in\mathbb{R}^2/\Gamma \tag{44}$$

Theorem 4.3
If $(\mathbf{u}, p)$ is given by (20) and (21), $(\mathbf{u}_h, p_h)$ is given by (43) and (44), then we have a constant C independent of h such that

$$\begin{aligned}&\|(\mathbf{u}-\mathbf{u}_h, p-p_h)\|_{(H^1(\Omega))^2\times(L^2(\Omega)/\mathbb{R})} + \|(\mathbf{u}-\mathbf{u}_h, p-p_h)\|_{(W_0^1(\Omega'))^2\times L^2(\Omega')}\\ &\leqslant Ch^{m+3/2}\|q\|_{H^{m+1}(\Gamma)/\mathbb{R}}, \quad 0\leqslant m\leqslant\gamma\end{aligned} \tag{45}$$

Proof
According to the arguments in Section 3.1, we actually know that (20) defined an isomorphism from $H_{00}^{-1/2}(\Gamma)$ onto $H^1(\Omega)\cup W_0^1(\Omega')$, and (21) defined an isomorphism from $H_{00}^{-1/2}(\Gamma)$ onto $(L^2(\Omega)/\mathbb{R})\cup L^2(\Omega')$. Thus, using Theorem 4.1 we have

$$\|u_i-u_{hi}\|_{H^1(\Omega)}\leqslant C\|q-q_h\|_{H^{-1/2}(\Gamma)/\mathbb{R}}\leqslant Ch^{m+3/2}\|q\|_{H^{m+1}(\Gamma)/\mathbb{R}}, \quad i=1,2$$

$$\|p-p_h\|_{L^2(\Omega)/\mathbb{R}}\leqslant C\|q-q_h\|_{H^{-1/2}(\Gamma)/\mathbb{R}}\leqslant Ch^{m+3/2}\|q\|_{H^{m+1}(\Gamma)/\mathbb{R}}$$

Similarly, the same inequalities with Ω' as above can be obtained. By gathering these estimates we end the proof. □

DOI: 10.1002/fld

Theorem 4.4
For $\forall \mathbf{y} \in \mathbb{R}^2$ with $d(\mathbf{y}, \Gamma) = \min_{\mathbf{x}\in\Gamma}\{|\mathbf{x}-\mathbf{y}|\} \geqslant \delta$, we have

$$|\partial^{\lambda}\mathbf{u}(\mathbf{y}) - \tilde{\partial}^{\lambda}\mathbf{u}_h(\mathbf{y})| \leqslant C\left(\sum_{l=0}^{\gamma+2}(d(\mathbf{y},\Gamma))^{-l-|\lambda|}\right)h^{m+\gamma+3}\|q\|_{H^{m+1}(\Gamma)/\mathbb{R}} \tag{46}$$

$$|\partial^{\lambda}p(\mathbf{y}) - \tilde{\partial}^{\lambda}p_h(\mathbf{y})| \leqslant C\left(\sum_{l=0}^{\gamma+2}(d(\mathbf{y},\Gamma))^{-l-|\lambda|}\right)h^{m+\gamma+3}\|q\|_{H^{m+1}(\Gamma)/\mathbb{R}} \tag{47}$$

where $0 \leqslant m \leqslant \gamma$, $|\lambda| = \lambda_1 + \lambda_2 \geqslant 0$, C is a constant independent of h.

Proof
From (20) and (43) one gets

$$\begin{aligned} |u_i(\mathbf{y}) - u_{hi}(\mathbf{y})| &= \left|\sum_{j=1}^{2}\int_{\Gamma}(q(\mathbf{x}) - q_h(\mathbf{x}))U_{ij}(\mathbf{x},\mathbf{y})n_j(\mathbf{x})\,\mathrm{d}S_{\mathbf{x}}\right| \\ &\leqslant \|q - q_h\|_{H^{-\gamma-2}(\Gamma)/\mathbb{R}}\sum_{j=1}^{2}\|U_{ij}n_j\|_{H_0^{\gamma+2}(\Gamma)}, \quad i = 1,2 \end{aligned} \tag{48}$$

Because of $d(\mathbf{y}, \Gamma) \geqslant \delta > 0$, we have

$$\sum_{j=1}^{2}\|U_{ij}(\mathbf{x},\mathbf{y})n_j(\mathbf{x})\|_{H_0^{\gamma+2}(\Gamma)} \leqslant C\sum_{j=1}^{2}\|U_{ij}(\mathbf{x},\mathbf{y})\|_{H^{\gamma+2}(\Gamma)} \leqslant C\sum_{l=0}^{\gamma+2}(d(\mathbf{y},\Gamma))^{-l} \tag{49}$$

Besides, it follows from Theorem 4.2 that

$$\|q - q_h\|_{H^{-\gamma-2}(\Gamma)/\mathbb{R}} \leqslant Ch^{m+\gamma+3}\|q\|_{H^{m+1}(\Gamma)/\mathbb{R}}, \quad 0 \leqslant m \leqslant \gamma \tag{50}$$

By gathering (48)–(50) we can prove (46) for $|\lambda| = 0$. Other cases are similar. □

Remark 4.2
Contrary to the case of the domain-type methods, such as the FEM, Theorem 4.4 indicates that the errors of $(\mathbf{u}, p)$ and their derivates in our Galerkin method are all of the same order.

Theorem 4.4 obtained the error of $(\mathbf{u}, p)$ and their derivatives outside the neighborhood of Γ; the following theorem will give the error inside the vicinity of the boundary.

Theorem 4.5
There exists $\delta > 0$, for $\forall \mathbf{y} \in \mathbb{R}^2$ with $d(\mathbf{y}, \Gamma) < \delta$ and for given $\varepsilon > 0$, we have

$$|\mathbf{u}(\mathbf{y}) - \mathbf{u}_h(\mathbf{y})| \leqslant C(\delta)h^{m+1-\varepsilon}\|q\|_{H^{m+1}(\Gamma)/\mathbb{R}}, \quad \varepsilon \leqslant m \leqslant \gamma$$

Proof
If $\varepsilon > 0$, one gets

$$|u_i(\mathbf{y}) - u_{hi}(\mathbf{y})| \leqslant \|q - q_h\|_{H^{\varepsilon}(\Gamma)/\mathbb{R}}\sum_{j=1}^{2}\|U_{ij}(\mathbf{x},\mathbf{y})n_j(\mathbf{x})\|_{H_0^{-\varepsilon}(\Gamma)}, \quad i = 1,2 \tag{51}$$

DOI: 10.1002/fld

Let $k=2/(1+\varepsilon)$, then $0<k<2$; thus, according to the Sobolev imbedding theorem, $L^2(\Gamma)\hookrightarrow L^k(\Gamma)\hookrightarrow H^{-\varepsilon}(\Gamma)$, so that

$$\begin{aligned}\sum_{j=1}^{2}\|U_{ij}(\mathbf{x},\mathbf{y})n_j(\mathbf{x})\|_{H_0^{-\varepsilon}(\Gamma)} &\leqslant C\sum_{j=1}^{2}\|U_{ij}(\mathbf{x},\mathbf{y})\|_{H^{-\varepsilon}(\Gamma)}\\ &\leqslant C\|\ln|\mathbf{x}-\mathbf{y}|\|_{H^{-\varepsilon}(\Gamma)}\\ &\leqslant C\|\ln|\mathbf{x}-\mathbf{y}|\|_{L^2(\Gamma)}\end{aligned}$$

Let $\Gamma^*=\{\mathbf{x}\in\Gamma:|\mathbf{x}-\mathbf{y}|<\delta\}$, $\ell_{\mathbf{y}}=\max_{\mathbf{x}\in\Gamma}|\mathbf{x}-\mathbf{y}|$, then

$$\begin{aligned}\|\ln|\mathbf{x}-\mathbf{y}|\|^2_{L^2(\Gamma)} &= \int_{\Gamma/\Gamma^*}|\ln|\mathbf{x}-\mathbf{y}||^2\,\mathrm{d}S_{\mathbf{x}}+\int_{\Gamma^*}|\ln|\mathbf{x}-\mathbf{y}||^2\,\mathrm{d}S_{\mathbf{x}}\\ &\leqslant \int_{\Gamma/\Gamma^*}(\max\{|\ln\ell_{\mathbf{y}}|,|\ln\delta|\})^2\,\mathrm{d}S_{\mathbf{x}}\\ &\quad+\delta|\ln\delta|^2+2\delta|\ln\delta|+2\int_{\Gamma^*}\mathrm{d}S_{\mathbf{x}}\\ &\leqslant \mathrm{mes}(\Gamma)(\max\{|\ln\ell_{\mathbf{y}}|,|\ln\delta|\})^2\\ &\quad+\delta|\ln\delta|^2+2\delta|\ln\delta|+2\,\mathrm{mes}(\Gamma)\end{aligned}$$

so

$$\sum_{j=1}^{2}\|U_{ij}(\mathbf{x},\mathbf{y})n_j(\mathbf{x})\|_{H_0^{-\varepsilon}(\Gamma)}\leqslant C(\delta) \tag{52}$$

Besides, using the triangle inequality yields

$$\|q-q_h\|_{H^{\varepsilon}(\Gamma)/\mathbb{R}}\leqslant\|q-S_hq\|_{H^{\varepsilon}(\Gamma)/\mathbb{R}}+\|S_hq-q_h\|_{H^{\varepsilon}(\Gamma)/\mathbb{R}}$$

On the one hand, according to Property 2.3, Theorem 2.1, and (37) we have

$$\begin{aligned}\|q-S_hq\|_{H^{\varepsilon}(\Gamma)/\mathbb{R}} &\leqslant \|q-\mathscr{M}q\|_{H^{\varepsilon}(\Gamma)/\mathbb{R}}+\|\mathscr{M}q-S_hq\|_{H^{\varepsilon}(\Gamma)/\mathbb{R}}\\ &\leqslant \|q-\mathscr{M}q\|_{H^{\varepsilon}(\Gamma)/\mathbb{R}}+Ch^{-\varepsilon}\|\mathscr{M}q-S_hq\|_{H^0(\Gamma)/\mathbb{R}}\\ &\leqslant \|q-\mathscr{M}q\|_{H^{\varepsilon}(\Gamma)/\mathbb{R}}\\ &\quad+Ch^{-\varepsilon}\{\|\mathscr{M}q-q\|_{H^0(\Gamma)/\mathbb{R}}+\|q-S_hq\|_{H^0(\Gamma)/\mathbb{R}}\}\\ &\leqslant Ch^{m+1-\varepsilon}\|q\|_{H^{m+1}(\Gamma)/\mathbb{R}},\quad \varepsilon\leqslant m\leqslant\gamma\end{aligned}$$

and, on the other hand, from Property 2.3, Theorem 4.1, and (38) we also have

$$\begin{aligned}\|S_hq-q_h\|_{H^{\varepsilon}(\Gamma)/\mathbb{R}} &\leqslant Ch^{-1/2-\varepsilon}\|S_hq-q_h\|_{H^{-1/2}(\Gamma)/\mathbb{R}}\\ &\leqslant Ch^{-1/2-\varepsilon}(\|S_hq-q\|_{H^{-1/2}(\Gamma)/\mathbb{R}}+\|q-q_h\|_{H^{-1/2}(\Gamma)/\mathbb{R}})\\ &\leqslant Ch^{m+1-\varepsilon}\|q\|_{H^{m+1}(\Gamma)/\mathbb{R}},\quad \varepsilon\leqslant m\leqslant\gamma\end{aligned}$$

DOI: 10.1002/fld

Thus

$$\|q-q_h\|_{H^{\varepsilon}(\Gamma)/\mathbb{R}} \leqslant Ch^{m+1-\varepsilon}\|q\|_{H^{m+1}(\Gamma)/\mathbb{R}}, \quad \varepsilon \leqslant m \leqslant \gamma \tag{53}$$

The proof is completed via collecting (51)–(53). □

Remark 4.3

We have no error estimates of $\partial\mathbf{u}/\partial\mathbf{n}$ and p in the vicinity of the boundary. That is because they are discontinuous through Γ.

5. NUMERICAL EXPERIMENTS

In this section, we present some numerical experiments to demonstrate the accuracy and efficiency of the proposed meshless method. In all examples, we use uniform particle distribution. For simplicity, we always assume that the viscosity of the fluid is taken as one. Besides, the polynomial basis is chosen as a quadratic basis, and the weight function is a cubic spline function [11]

$$w_i(\mathbf{x}) = \begin{cases} \frac{2}{3} - 4d^2 + 4d^3, & d \leqslant \frac{1}{2} \\ 4/3 - 4d + 4d^2 - 4d^3/3, & \frac{1}{2} < d \leqslant 1 \\ 0, & d > 1 \end{cases}$$

where $d = |\mathbf{x}-\mathbf{x}_i|/h$, h is the radius of the weight functions. In all examples, h is taken to be $3.5\bar{d}$, with $\bar{d}$ as the nodal spacing.

5.1. Flow between two parallel plates

Consider a unidirectional flow between two parallel plates (Figure 1). The fluid is subjected to a step pressure differential, $p = p_0(1-x_1/L)$. The x_2-component velocity vanishes everywhere, $u_2 = 0$, and the x_1-component velocity is a function of x_2 only, $u_1 = u_1(x_2)$. With these conditions, the analytical solution can be given by [36] as

$$u_1(x_2) = \frac{p_0 b}{2L\mu} x_2 \left(1 - \frac{x_2}{b}\right)$$

The problem is solved as a 2-D problem with slip boundary conditions. Although the solution in dimensionless form is independent of the geometry, a rectangle domain of $L = 2b$ and $b = \sqrt{2}$ is chosen. Besides, the parameter p_0 is equal to L.

Figure 2 displays a comparison between the present numerical results with the exact solutions for the x_1-component velocity and its derivatives. In this analysis, we applied 24 boundary nodes. The node distribution on the rectangle domain is as shown in Figure 1. It is evident that the results agree well with the analytical solution.

To show the convergence of the presented method, regularly distributed 12, 24, 48, and 96 nodes are used. In this study, the ratio of the number of nodes on A_1A_2 and A_3A_4 to that on A_1A_4 and A_2A_3 is kept constant and equal to two. The results of convergence of ($\mathbf{u}$, p) are shown in Figure 3. It is observed that the numerical rate matches our theoretical result.

For investigating the behavior of points far away from the boundary and near the boundary, the values of the numerical approximations of ($\mathbf{u}$, p) and their derivates at some inner points are given

DOI: 10.1002/fld

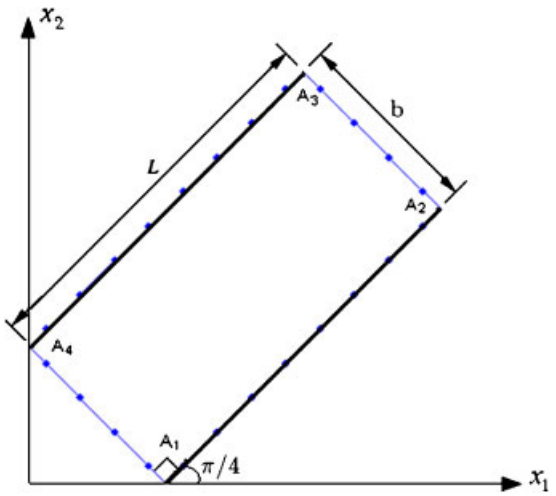

Figure 1. Steady flow between two parallel plates.

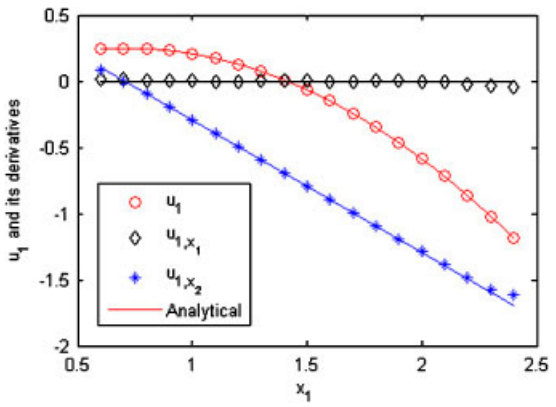

Figure 2. Results of u_1 and its derivates along the line $x_1 = x_2$.

in Table I. The results show that the error decreases with the increase of the boundary nodes. The numerical convergence rates of $(\mathbf{u}, p)$ and their derivates match our theoretical results for points far away from the boundary. While points lie in the neighborhood of Γ, the numerical results of $\mathbf{u}$ also confirm the theoretical error statements.

5.2. *Flow around a rectangular cylinder between two parallel plates*

In this example, we solve the problem of fluid flow around an infinitely long rectangular cylinder and in the middle of the channel bounded by two parallel plates (see Figure 4). Because of symmetry, only one-quarter of the problem domain is taken into consideration. For ease of comparison, the geometry is chosen as $L_1 = L_2 = 2$, $b_1 = b_2 = 1$ and, in addition, the exact solution for this

DOI: 10.1002/fld

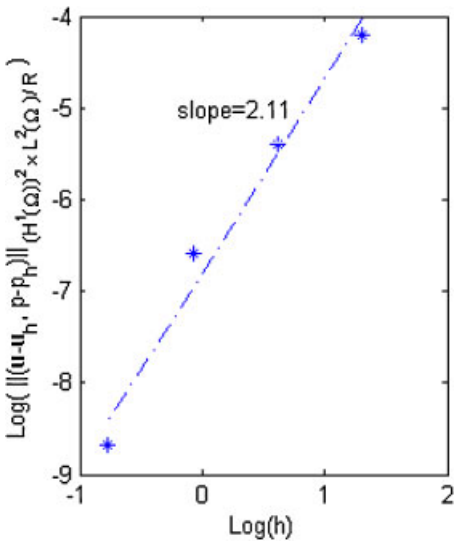

Figure 3. Convergence of flow between two parallel plates.

Table I. Approximations and convergence rates for parallel plates flow.

		Numerical solutions					
x_1, x_2		$N=12$	$N=24$	$N=48$	$N=96$	Exact	Rates
1.5, 2.1	u_1	−0.697146	−0.721421	−0.720031	−0.720110	−0.720076	3.31
	u_{1,x_1}	−0.031335	−0.018834	−0.000113	−0.000107	0.000000	3.20
	u_{1,x_2}	−1.337429	−1.422490	−1.388958	−1.392828	−1.392893	3.21
	u_2	−0.023988	0.002745	−0.000286	−0.000025	0.000000	3.30
	u_{2,x_1}	0.042903	−0.012094	0.003236	−0.000035	0.000000	3.26
	u_{2,x_2}	0.031335	0.018833	0.000113	0.000107	0.000000	3.20
	$p_{,x_1}$	−1.450490	−1.045208	−1.015424	−1.000033	−1.000000	4.27
	$p_{,x_2}$	0.711135	−0.218806	0.022114	−0.000013	0.000000	5.04
2.0, 1.100	u_1	0.178116	0.175553	0.172171	0.172799	0.172817	2.65
2.0, 1.050	u_1	0.209352	0.193522	0.191859	0.191084	0.191212	2.33
2.0, 1.010	u_1	0.217676	0.211757	0.207264	0.203890	0.204128	1.88
2.0, 1.005	u_1	0.217715	0.210951	0.207391	0.206622	0.205630	1.24

problem is

$$u_1 = x_1(x_1^2 + 2x_1 + 3x_2^2) + 2(x_2 - 1)^2 + \tfrac{8}{3}$$

$$u_2 = -x_2(3x_1^2 + 4x_2 + x_2^2) + 4x_1 + 2$$

$$p = 6(x_1^2 - x_2^2) + 8x_1 + p_0$$

where p_0 is a constant. Along the channel walls and the rectangular cylinder surface, the slip conditions are prescribed.

DOI: 10.1002/fld

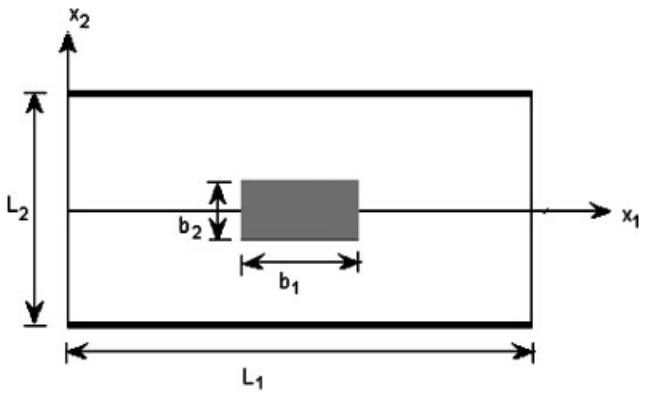

Figure 4. Flow around a rectangular cylinder between two parallel plates.

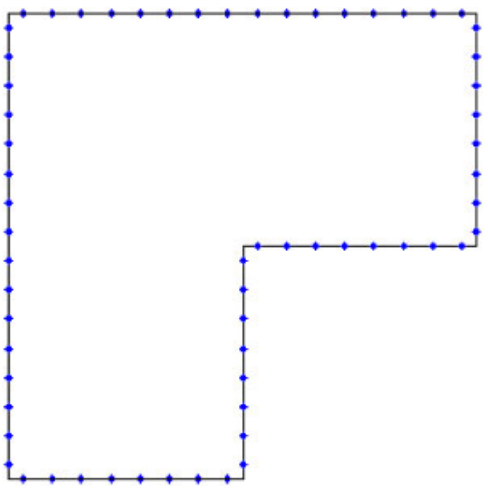

Figure 5. Arrangement of nodes.

The node distribution is as shown in Figure 5. In this analysis, we applied 64 boundary nodes. The comparison of the exact solutions and numerical solutions for $(\mathbf{u}, p)$ and their derivates are plotted in Figures 6–8. The numerical solutions are seen to capture the behavior of the exact solutions very well. We remark that the pressure is only determined up to a constant, and in this case $p_0 = 4.8468$. Besides, the velocity field inside the solution domain is plotted in Figure 9 and shows the correct fluid motion. Moreover, Figure 10 depicts the computed results of the contour of pressure.

When four different regular node arrangements of 8, 16, 32, and 64 nodes have been used, the convergence rates are plotted with respect to Sobolev norms in Figure 11. It is true that the numerical rates match our theoretical results.

The values of the numerical results of $(\mathbf{u}, p)$ and their derivates at some inner points far away from the boundary are displayed in Table II. Besides, the numerical solutions of the x_1-component

DOI: 10.1002/fld

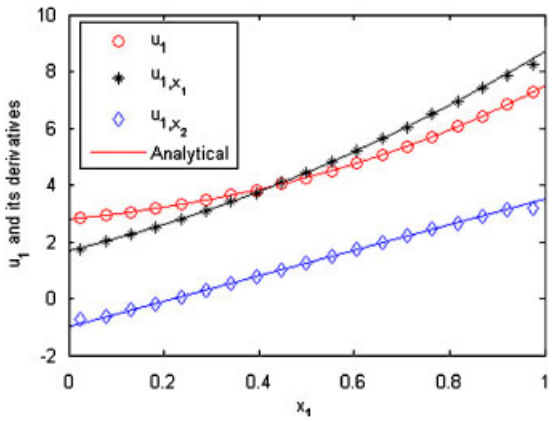

Figure 6. Results of u_1 and its derivates along the line $x_2 = 0.75$.

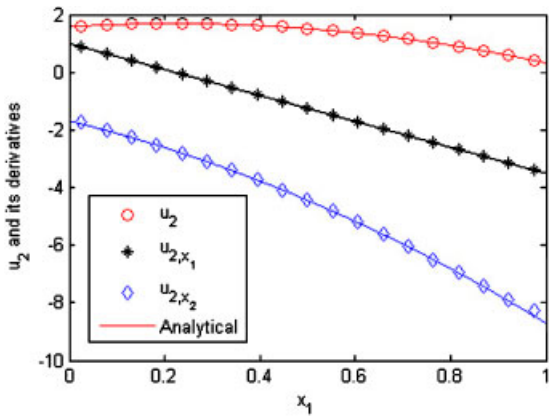

Figure 7. Results of u_2 and its derivates at the section $x_2 = 0.75$.

velocity at points near the boundary are shown in Table III. As we expected, the results from the proposed meshless method gradually converge to the exact values along with the decrease of the radii of the weight functions, and the numerical results also confirm theoretical analysis.

6. CONCLUSIONS

In this study, we have developed a meshless Galerkin method for direction solution of 2-D incompressible slip Stokes flows. It is a boundary-type meshless method, which combines scattered points and BIEs. The main attractive features of this methodology are the following:

(1) The simple layer potential used for the Stokes problem is combined with the slip boundary condition. This fact leads to a set of BIEs of the first kind and the problem of finding velocity and that of finding pressure can be separated. Besides, the expressions of the velocity and

DOI: 10.1002/fld

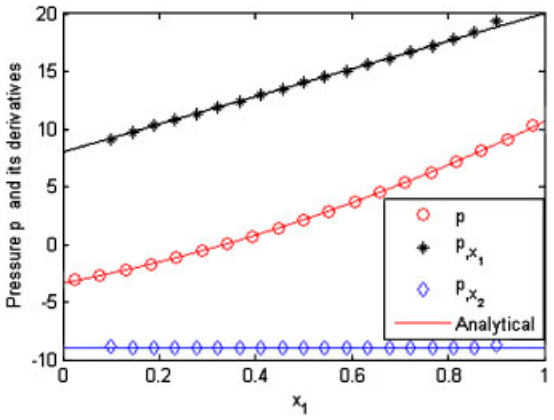

Figure 8. Pressure p and its derivates along $x_2 = 0.75$.

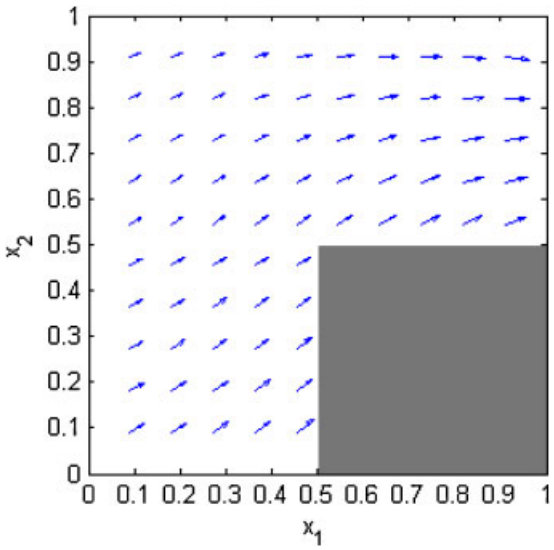

Figure 9. Velocity vectors.

the pressure are suitable for the interior as well as the exterior problems. Thus compared with the domain-type methods, such as the EFGM, the RKPM, and the LBIE method, the new approach reduces the dimensionality of the original problem.

(2) The numerical analysis is based on the variational formulation of BIEs. Thus, implementing boundary conditions in this method is much easier than that in other meshless methods, such as in the BNM, the BCM, and the EFGM, in which the MLS is introduced also. Besides, the system matrices are symmetric, which provides an added advantage in coupling this method with the FEM or other domain-type meshless methods for the problems with unbounded domain.

DOI: 10.1002/fld

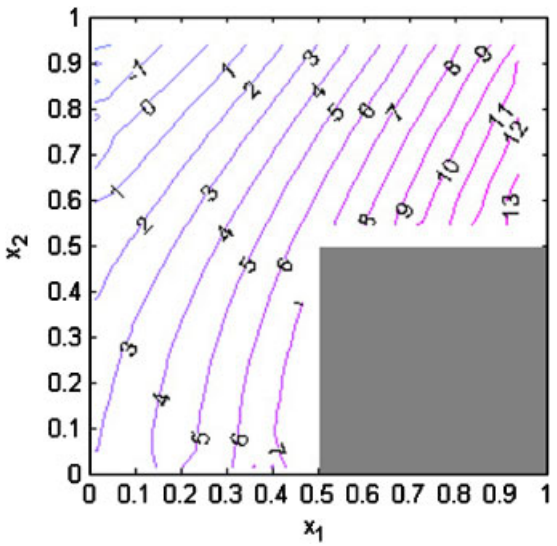

Figure 10. Pressure contour.

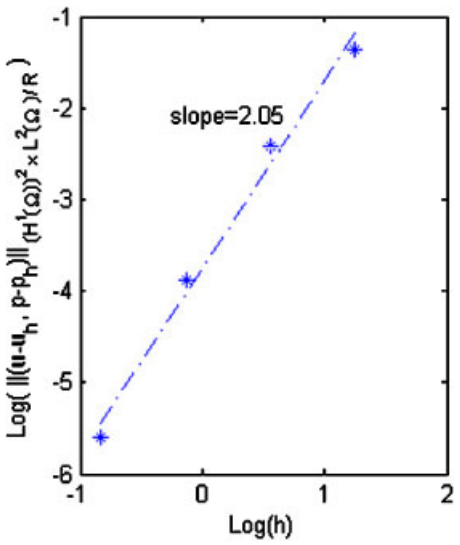

Figure 11. The convergence rate.

(3) For tackling constraint conditions of trial functions, a Lagrangian multiplier is introduced in the process of numerical approximation.
(4) The MLS approximations are used to generate trial and test functions. This technique leads to the fact that the proposed method is a meshless method, which only requires a nodal data structure on the bounding surface of the domain to be solved.

DOI: 10.1002/fld

Table II. Approximations of $(\mathbf{u}, p)$ for points far away from the boundary.

		Numerical solutions					
x_1, x_2		$N=8$	$N=16$	$N=32$	$N=64$	Exact	Rates
0.15, 0.40	u_1	3.571248	3.488134	3.506673	3.507107	3.507042	3.55
	u_{1,x_1}	1.799914	1.213746	1.156641	1.148231	1.147500	3.23
	u_{1,x_2}	−3.194040	−2.044789	−2.048093	−2.040184	−2.040000	3.71
	u_2	2.253723	2.260139	2.269347	2.269025	2.269000	3.24
	u_{2,x_1}	2.736017	2.041131	2.033679	2.039720	2.040000	3.14
	u_{2,x_2}	−1.799914	−1.213746	−1.156641	−1.148231	−1.147500	3.23
	$p_{,x_1}$	6.745009	12.20920	9.937532	9.802540	9.800000	3.48
	$p_{,x_2}$	−9.274094	−4.409383	−4.927565	−4.804245	−4.800000	3.17
0.70, 0.75	u_1	5.630939	5.263234	5.295569	5.296119	5.295917	3.86
	u_{1,x_1}	7.514424	5.837650	5.925785	5.956544	5.957500	3.39
	u_{1,x_2}	2.217436	2.228257	2.160985	2.149993	2.150000	4.25
	$p_{,x_1}$	2.890770	20.97290	16.23293	16.38105	16.40000	3.32
	$p_{,x_2}$	−6.414485	−10.03502	−9.006113	−8.994141	−9.000000	3.38

Table III. Approximations of u_1 for points near the boundary.

	Numerical solutions					
x_1, x_2	$N=8$	$N=16$	$N=32$	$N=64$	Exact	Rates
0.1000, 0.5	3.183692	3.260215	3.264074	3.262708	3.262667	3.35
0.0100, 0.5	3.111812	3.188223	3.176271	3.173834	3.174368	2.35
0.0010, 0.5	3.114021	3.195793	3.180477	3.171381	3.167419	1.24
0.0001, 0.5	3.113416	3.195641	3.180238	3.171373	3.166742	1.17

The error estimates for the proposed method in Sobolev spaces have been presented, which show that the error bound of the numerical solution is directly related to the radii of the weight functions. Besides, velocity, pressure, and their successive derivatives possess L^∞-superconvergence outside the neighborhood of Γ. Moreover, we have got the convergence of velocity in L^∞ norm in the vicinity of Γ.

Some examples have been given and the numerical results are accurate and are in agreement with the theoretical orders of convergence. The proposed method can be extended to solve nonlinear or non-stationary problems by reducing them to linear and stationary ones with the help of perturbation and time-stepping procedures.

REFERENCES

1. Saito H, Scriven LE. Study of coating flow by the finite element method. *Journal of Computational Physics* 1981; **42**:53–76.
2. Verfurth H. Finite element approximation of incompressible Navier–Stokes equations with slip boundary condition. *Numerische Mathematik* 1987; **50**:697–721.
3. Georgios CG, Lorraine GO, William WS, Susan S. A singular finite element for Stokes flow: the stick-slip problem. *International Journal for Numerical Methods in Fluids* 1989; **9**:1353–1367.

DOI: 10.1002/fld

4. Kistler SF, Scriven LE. Coating flow theory by finite element and asymptotic analysis of the Navier–Stokes system. *International Journal for Numerical Methods in Fluids* 1984; **4**:207–229.
5. Braess H, Wriggers P. Arbitrary Lagrangian Eulerian finite element analysis of free surface flow. *Computer Methods in Applied Mechanics and Engineering* 2000; **190**:95–109.
6. Hebeker FK. An integral equation of the first kind for a free boundary value problem of the stationary Stokes' equations. *Mathematical Methods in the Applied Sciences* 1987; **9**:550–575.
7. Zhu J, Jin C. Boundary element approximation of Stokes equation with slip boundary condition. In *Boundary Elements X*, Brebbia CA (ed.), vol. 2. Computational Mechanics Institute: Southampton, Boston, 1988; 301–308.
8. Reidinger B, Steinbach O. A symmetric boundary element method for the Stokes problem in multiple connected domains. *Mathematical Methods in the Applied Sciences* 2003; **26**:77–93.
9. Ding J, Ye W. A fast integral approach for drag force calculation due to oscillatory slip stokes flows. *International Journal for Numerical Methods in Engineering* 2004; **60**:1535–1567.
10. Yu D. *Natural Boundary Integral Method and its Applications*. Kluwer: Boston, 2002.
11. Belytschko T, Krongauz Y, Organ D, Fleming M. Meshless methods: an overview and recent developments. *Computer Methods in Applied Mechanics and Engineering* 1996; **139**:3–47.
12. Liu GR. *Meshfree Methods—Moving Beyond the Finite Element Method*. CRC: Boca Raton, 2002.
13. Li S, Liu WK. *Meshfree Particle Methods*. Springer: Berlin, 2004.
14. Belytschko T, Krysl P, Krongauz Y. A three-dimensional explicit element-free galerkin method. *International Journal for Numerical Methods in Fluids* 1997; **24**:1253–1270.
15. Han W, Meng X. Error analysis of the reproducing kernel particle method. *Computer Methods in Applied Mechanics and Engineering* 2001; **190**:6157–6181.
16. Christon MA, Voth TE. Results of von Neumann analyses for reproducing kernel semi-discretizations. *International Journal for Numerical Methods in Engineering* 2000; **47**:1285–1301.
17. Liu WK, Li S, Belytschko T. Moving least-square reproducing kernel methods (I) methodology and convergence. *Computer Methods in Applied Mechanics and Engineering* 1997; **143**:113–154.
18. Strouboulis T, Copps K, Babuska I. The generalized finite element method. *Computer Methods in Applied Mechanics and Engineering* 2001; **190**:4081–4196.
19. Cheng M, Liu GR. A novel finite point method for flow simulation. *International Journal for Numerical Methods in Fluids* 2002; **39**:1161–1178.
20. Liu GR, Gu YT. A point interpolation method for two-dimensional solids. *International Journal for Numerical Methods in Engineering* 2001; **50**:937–951.
21. Duarte CA, Oden JT. *H-p* clouds—an *h–p* meshless method. *Numerical Methods for Partial Differential Equations* 1996; **12**:675–705.
22. Zhang XK, Kwon KC, Youn SK. Least-squares meshfree method for incompressible Navier–Stokes problems. *International Journal for Numerical Methods in Fluids* 2004; **46**:263–288.
23. Atluri SN, Sladek J, Sladek V, Zhu T. The local boundary integral equation (LBIE) and it's meshless implementation for linear elasticity. *Computational Mechanics* 2000; **25**:180–198.
24. Mukherjee YX, Mukherjee S. The boundary node method for potential problems. *International Journal for Numerical Methods in Engineering* 1997; **40**:797–815.
25. Kothnur VS, Mukherjee S, Mukherjee YX. Two-dimensional linear elasticity by the boundary node method. *International Journal of Solids and Structures* 1999; **36**:1129–1147.
26. Li G, Aluru NR. Boundary cloud method: a combined scattered point/boundary integral approach for boundary-only analysis. *Computer Methods in Applied Mechanics and Engineering* 2002; **191**:2337–2370.
27. Gu YT, Liu GR. A boundary point interpolation method for stress analysis of solids. *Computational Mechanics* 2002; **28**:47–54.
28. Atluri SN, Shen SP. The meshless local Petrov–Galerkin (MLPG) method: a simple & less-costly alternative to the finite element and boundary element methods. *Computer Modeling in Engineering and Sciences* 2002; **3**:11–51.
29. Lancaster P, Salkauskas K. Surface generated by moving least squares methods. *Mathematics of Computation* 1981; **37**:141–158.
30. Ladyzhenskaya OA. *The Mathematical Theory of Viscous Incompressible Flow*. Gordon and Breach: New York, 1969.
31. Dautray R, Lious JL, Artola M, Benilan P. *Mathematical Analysis and Numerical Methods for Science and Technology*, *Volume 4*: *Integral Equations and Numerical Methods*. Springer: Berlin, 2000.

DOI: 10.1002/fld

32. Brezzi F. On the existence, uniqueness and approximation of saddle-point problems arising from Lagrange multipliers. *RAIRO Analyse Numérique* 1974; **R2**:129–151.
33. Girault V, Raviart PA. *Finite Element Approximation of the Navier–Stokes Equations*. Springer: Berlin, 1979.
34. Lious JL, Magenes E. *Non-homogeneous Boundary Value Problems and Applications*. Springer: Berlin, 1972.
35. Zuppa C. Error estimates for moving least-square approximations. *Bulletin Brazilian Mathematical Society*, *New Series* 2003; **34**:231–249.
36. Carslaw HS, Jaeger JC. *Conduction of Heat in Solids*. Oxford University Press: New York, 1956.

DOI: 10.1002/fld